THE JOURNAL OF BIOLOGICAL CHEMISTRY VOL. 286, NO. 19, pp. 17205–17216, May 13, 2011

Critical Role of the β-Subunit CDC50A in the Stable Expression, Assembly, Subcellular Localization, and Lipid Transport Activity of the P_4-ATPase ATP8A2*[S]

Received for publication, February 10, 2011, and in revised form, March 14, 2011 Published, JBC Papers in Press, March 18, 2011, DOI 10.1074/jbc.M111.229419

Jonathan A. Coleman[‡1] **and Robert S. Molday**[‡§2]

From the Departments of [‡]*Biochemistry and Molecular Biology and* [§]*Ophthalmology and Visual Sciences, Centre for Macular Research, University of British Columbia, Vancouver, British Columbia V6T 1Z3, Canada*

P_4-ATPases have been implicated in the transport of lipids across cellular membranes. Some P_4-ATPases are known to associate with members of the CDC50 protein family. Previously, we have shown that the P_4-ATPase ATP8A2 purified from photoreceptor membranes and reconstituted into liposomes catalyzes the active transport of phosphatidylserine across membranes. However, it was unclear whether ATP8A2 functioned alone or as a complex with a CDC50 protein. Here, we show by mass spectrometry and Western blotting using newly generated anti-CDC50A antibodies that CDC50A is associated with ATP8A2 purified from photoreceptor membranes. ATP8A2 expressed in HEK293T cells assembles with endogenous or expressed CDC50A, but not CDC50B, to generate a heteromeric complex that actively transports phosphatidylserine and to a lesser extent phosphatidylethanolamine across membranes. Chimera CDC50 proteins in which various domains of CDC50B were replaced with the corresponding domains of CDC50A were used to identify domains important in the formation of a functional ATP8A2-CDC50 complex. These studies indicate that both the transmembrane and exocytoplasmic domains of CDC50A are required to generate a functionally active complex. The N-terminal cytoplasmic domain of CDC50A appears to play a direct role in the reaction cycle. Mutagenesis studies further indicate that the *N*-linked oligosaccharide chains of CDC50A are required for stable expression of an active ATP8A2-CDC50A lipid transport complex. Together, our studies indicate that CDC50A is the β-subunit of ATP8A2 and is crucial for the correct folding, stable expression, export from endoplasmic reticulum, and phosphatidylserine flippase activity of ATP8A2.

P_4-ATPases comprise a subfamily of P-type ATPases implicated in the active transport or flipping of aminophospholipids from the exocytoplasmic to the cytoplasmic side of cell membranes (1–6). This activity generates and maintains aminophospholipid asymmetry, which plays a crucial role in such cellular processes as membrane stability and impermeability, vesicle-mediated protein transport, blood coagulation, establishment of cellular polarity, recognition of apoptotic cells, cellular division, sperm capacitation, and regulation of membrane protein function (7–9). The importance of P_4-ATPases is highlighted by the finding that mutations in several P_4-ATPases including ATP8B1 and ATP8A2 have been linked to severe human diseases (10–13).

A number of yeast, plant, and mammalian P_4-ATPases are known to associate with members of the Cdc50 family of proteins (14–17). There are three members of this family in yeast (Cdc50p, Crflp, and Lem3/Ros3p) and three in mammals (CDC50A, CDC50B, and CDC50C). These proteins contain two transmembrane segments separated by a relatively large glycosylated exocytoplasmic domain. Several cellular studies indicate that CDC50 proteins play a crucial role in the export of specific P_4-ATPases from the ER of cells (14–19). CDC50 proteins also have been suggested to play a direct role in the reaction cycle of P_4-ATPases (20, 21). In yeast, the P_4-ATPase Drs2p requires Cdc50p for phosphorylation of the key aspartate residue involved in the ATPase catalytic reaction. The affinity of Drs2p for Cdc50p was also found to change during the transport cycle. Additionally, phosphorylation of the catalytically important aspartate residue of the human P_4-ATPases, ATP8B1 and ATP8B2, was dependent on the CDC50 subunit. On the basis of these studies, it has been proposed that the CDC50 proteins serve as the β-subunit of P_4-ATPases akin to the β-subunit of the Na^+/K^+ ATPase (9). However, although an association between the catalytic subunit of P_4-ATPases and CDC50 proteins has been observed in heterologous cell expression systems, their direct association in mammalian tissues has not been demonstrated, and the domains of CDC50 proteins responsible for their interaction with P_4-ATPases have yet to be determined.

Recently, we have purified, localized, and characterized the functional properties of mammalian ATP8A2, a member of the P_4-ATPase family that shares a 67% amino acid sequence identity with ATP8A1, the founding member of mammalian P_4-ATPases (5). *ATP8A2* expression was detected in the retina, testes, and brain (5, 13). In the retina, ATP8A2 is localized in the outer segment compartment of rod and cone photoreceptors

* This work was supported by Canadian Institutes of Health Research Grant MOP-106667.

[S] The on-line version of this article (available at http://www.jbc.org) contains supplemental Tables S1 and S2 and Figs. S1–S4.

[1] Supported by a University of British Columbia and National Sciences and Engineering Council predoctoral studentship.

[2] Canada Research Chair in Vision and Macular Degeneration. To whom correspondence should be addressed: Dept. of Biochemistry and Molecular Biology, 2350 Health Sciences Mall, University of British Columbia, Vancouver, British Columbia V6T 1Z3, Canada. Tel.: 604-822-6173; Fax: 604-822-5227; E-mail: molday@interchange.ubc.ca.

where it functions in the transport of PS[3] and to a lesser extent PE across the photoreceptor disc membrane (5). In a proteomic study, unique peptides belonging to CDC50A were detected in photoreceptor outer segment preparations (22), but the possible association of CDC50A with ATP8A2 was not investigated.

In this study, we show that ATP8A2 is present as a heteromeric complex with CDC50A in photoreceptor outer segments as well as HEK293T cells expressing ATP8A2. Co-expression of ATP8A2 with CDC50A, but not CDC50B, not only promotes the translocation of ATP8A2 from the endoplasmic reticulum (ER) to the Golgi but also significantly enhances the yield of a functional ATP8A2-CDC50A aminophospholipid transporter. Chimera proteins in which various domains of CDC50B have been replaced with corresponding domains of CDC50A have been used to define regions of CDC50A that are required for the formation of a functionally active ATP8A2-CDC50A complex. Finally, we have investigated the effect of *N*-linked glycosylation of CDC50A on the stable expression, subunit association, and functional properties of the ATP8A2-CDC50A complex.

EXPERIMENTAL PROCEDURES

Materials—1,2-Dioleoyl-*sn*-glycero-3-phospho-ethanolamine, 1,2-dioleoyl-*sn*-glycero-3-phosphoserine, L-α-phosphatidylcholine (egg, chicken), C6 NBD-PS, C6 NBD-PE, and C6 NBD-PC were purchased from Avanti Polar Lipids (Alabaster, AL). ATP, AMP-PNP, sodium orthovanadate, and *n*-octyl-β-D-glucopyranoside were purchased from Sigma, dithionite was from Fisher (Waltham, MA), CHAPS was from Anatrace (Maumee, OH), and the synthetic 6C11 and 7F4 peptides, Ac-RDRLLKRLS and Ac-AKDEVDGGP, respectively, were purchased from Biomatik (Cambridge, Canada). Complete inhibitor was from Roche Applied Science. The Rho 1D4 antibody was obtained from UBC-UILO (Vancouver, Canada), and the 1D4 peptide was from the Nucleic Acid Protein Service Unit (Vancouver, Canada). The restriction enzymes were from New England Biolabs (Ipswich, MA). The primers were purchased from Integrated DNA Technologies (Coralville, IA).

Solutions—The compositions of the buffers were as follows: Buffer A: 50 mM HEPES, pH 7.5, 150 mM NaCl, 5 mM $MgCl_2$, 1 mM DTT, 20 mM CHAPS, 0.5 mg/ml egg PC, complete inhibitor; Buffer B: 50 mM HEPES, pH 7.5, 150 mM NaCl, 5 mM $MgCl_2$, 1 mM DTT, 10 mM CHAPS, 0.5 mg/ml egg PC; Buffer C, 50 mM HEPES, pH 7.5, 150 mM NaCl, 5 mM $MgCl_2$, 1 mM DTT, 0.75% *n*-octyl-β-D-glucopyranoside, 0.5 mg/ml egg PC; Buffer D: 50 mM HEPES, pH 7.5, 150 mM NaCl, 12.5 mM $MgCl_2$, 10 mM CHAPS, and 1 mM DTT; Buffer E: 50 mM HEPES, pH 7.5, 150 mM NaCl, 5 mM $MgCl_2$, 1 mM DTT, 1% *n*-octyl-β-D-glucopyranoside, 5 mg/ml egg PC, 10% sucrose; Buffer F: 10 mM HEPES, pH 7.5, 150 mM NaCl, 5 mM $MgCl_2$, 1 mM DTT, 10% sucrose; and PBS: 10 mM phosphate, pH 7.4, 140 mM NaCl, 3 mM KCl.

DNA Constructs—Bovine *Atp8a2* containing a 1D4 tag in pcDNA3 (Invitrogen) was described previously (5). This construct was used as a PCR template to generate each *Atp8a2* construct described. The cDNA of bovine *Cdc50a* (IMAGE: 8284976) and human *Cdc50b* (IMAGE: 8322611) were purchased from Open Biosystems (Huntsville, AL). Restriction sites and epitope tags were introduced by PCR. Full-length *Atp8a2* without a tag was PCR-amplified and cloned into pcDNA3 using BamHI and NotI restriction sites. Full-length *Cdc50a* with a 1D4 or Myc tag was cloned into pcDNA3 using the HindIII and XhoI restrictions sites. *Cdc50b* with a 1D4 tag was also cloned into pcDNA3 using HindIII and XhoI sites. The 1D4-tagged constructs contained a 9-amino acid C-terminal tag (TETSQVAPA). The Myc-tagged constructs contained a 10-amino acid C-terminal tag (EQKLISEEDL). Chimeras of *Cdc50a* and *Cdc50b* were constructed from a 1D4-tagged *Cdc50b* construct that had been cloned into a modified pcDNA3 vector by EcoRI and NotI. Silent restriction sites were inserted into *Cdc50b* by mutagenesis to facilitate cloning of individual domains. The ECD chimera contained amino acids 1–57 and 301–351 of CDC50B and amino acids 73–308 of CDC50A. The ECD/TM chimera contained amino acids 1–33 and 341–351 of CDC50B and amino acids 49–348 of CDC50A. The ECD/TM/C chimera contained amino acids 1–33 of CDC50B and amino acids 49–361 of CDC50A. The N-terminal chimera contained amino acids 1–47 of CDC50A and amino acids 33–351 of CDC50B. The M1 chimera contained amino acids 1–33 and 55–351 of CDC50B and amino acids 49–69 of CDC50A. The M2 chimera contained amino acids 1–301 and 341–351 of CDC50B and amino acids 310–348 of CDC50A. The M1/M2 chimera contained amino acids 1–33, 55–301, and 341–351 of CDC50B and amino acids 49–69 and 310–348 of CDC50A. GST fusion constructs containing amino acids 1–40 and 194–283 of CDC50A were cloned into pGEX-4T-1 (GE Healthcare) using the BamHI and EcoRI restriction sites. Site-directed mutations were created using the QuikChange mutagenesis kit from Agilent Technologies (Santa Clara, CA). All of the constructs were verified by DNA sequencing (Eurofins MWG Operon, Huntsville, AL).

Gene Expression by RT-PCR—RNA was isolated from tissues of 6-month-old C57/B6 mice and HEK293T cells (American Type Culture Collection, Manassas, VA) using the guanidinium thiocyanate phenol chloroform method (23). Random primed cDNA was made using the first strand cDNA synthesis kit (GE Healthcare). *Cdc50a*, *Cdc50b*, and *Cdc50c* gene expression was measured using gene specific primers. GapdH was used as a loading control. GapdH PCRs were run for 25 cycles. The *cdc50* genes were amplified for 25 cycles, and then 2 μl of the reaction was removed and reamplified for an additional 25 cycles. *Taq* polymerase (New England Biolabs) was used for amplification, and the primers were annealed at 55 °C. Primer sequences are available (supplemental Table S1).

Generation of Monoclonal Antibodies against CDC50A—Fragments of bovine CDC50A (amino acids 1–40 and 194–283) were cloned in frame with GST and expressed and purified from *Escherichia coli* BL21 on a glutathione-Sepharose-4B col-

[3] The abbreviations used are: PS, phosphatidylserine; PE, phosphatidylethanolamine; PC, phosphatidylcholine; ROS, rod outer segments; NBD, 7-nitrobenz-2-oxa-1,3-diazol-4-yl; NBD-PS, 1-oleoyl-2-{6-[7-nitro-2–1,3-benzoxadiazol-4-yl)amino]hexanoyl}-*sn*-glycero-3-phosphoserine; NBD-PE, 1-oleoyl-2-{6-[7-nitro-2–1,3-benzoxadiazol-4-yl)amino]hexanoyl}-*sn*-glycero-3-phosphoethanolamine; NBD-PC, 1-oleoyl-2-{6-[7-nitro-2–1,3-benzoxadiazol-4-yl)amino]hexanoyl}-*sn*-glycero-3-phosphocholine; AMP-PNP, adenylyl-imidodiphosphate; CHAPS, 3-[(3-cholamidopropyl)dimethylammonio]-1-propanesulfonic acid; ER, endoplasmic reticulum, TM, transmembrane; ECD, exocytoplasmic domain.

umn (GE Healthcare). Hybridoma cell lines were generated from Swiss Webster mice (Charles River, Wilmington, MA) immunized with a mixture of the GST fusion proteins as previously described (24). Positive clones were identified by screening for immunoreactivity against purified 1D4-tagged CDC50A protein expressed in HEK293T cells by ELISA. Immunoreactivity was confirmed on Western blots of bovine ROS. The epitope for the Cdc50–7F4 antibody was identified by measuring the reactivity of the antibody to a series of overlapping 9-amino acid N-terminal peptides using the SPOTs kit (Sigma).

Expression of ATP8A2 and CDC50A in HEK293T and Cos-7 Cells—The cells were maintained in Dulbecco's modified Eagle's medium supplemented with 10% fetal bovine serum, 100 units/ml penicillin, 100 μg/ml streptomycin, 2 mM L-glutamine, and 1.25 μg/ml fungizone. HEK293T cells in 10-cm dishes were transfected at 30% confluence with 10 μg of pcDNA3 containing either *Atp8a2* or *Cdc50a* by the calcium phosphate method (25) and harvested 48 h later. In some cases, the cells were co-transfected with both *Atp8a2* and *Cdc50a* by mixing 10 μg of each plasmid together followed by calcium phosphate precipitation. The membranes from HEK293T cells were prepared as described (26). Cos-7 cells (American Type Tissue Collection) were transfected in six-well plates containing polylysine-treated coverslips with 2.5 μg of each plasmid.

Immunofluorescence Microscopy—Cryosections of bovine retina tissue were prepared by fixing bovine eyes in 4% paraformaldehyde, 100 mM phosphate buffer, pH 7.4, for 1 h. Cryosections (10 μm) were cut followed by blocking and permeabilization with 10% normal goat serum and 0.2% Triton X-100 in phosphate buffer for 30 min. The sections were then labeled overnight at room temperature with Atp2F6 hybridoma supernatant diluted 2:3 in phosphate buffer containing 2.5% normal goat serum and 0.1% Triton X-100 or purified Cdc50–7F4 antibody at a concentration of 1 μg/ml. In control studies, Cdc50–7F4 antibody labeling was blocked by preabsorption with 7F4 peptide at a concentration of 0.2 μg/μl for 30 min. Cos-7 cells transfected with 1D4-tagged *Atp8a2* or Myc-tagged *Cdc50a* were labeled with either Rho-1D4 hybridoma culture fluid (1:500) or Myc antibody diluted 1:200 (ab10910; Abcam, Cambridge, MA). The cells were also labeled with antibodies against calnexin (Abcam, ab13504) or GM130 (Sigma; G7295) diluted 1:200 and 1:300, respectively. Cos-7 cells transfected with untagged *Atp8a2* and 1D4 tagged CDC50A chimeras were labeled with Atp2F6 and GM130 antibodies. The samples were washed with phosphate buffer and labeled for 1 h with Cy3- or Alexa-488 tagged goat anti-mouse Ig secondary antibody (diluted 1:1000) and counterstained with DAPI. Double labeling studies were performed with anti-mouse secondary and Alexa 568 goat anti-rat Ig, Alexa 594 goat anti-rabbit Ig, or Alexa 488 anti-rabbit (diluted 1:1000). The samples were examined on a Zeiss LSM 700 confocal scanning microscope.

Purification of ATP8A2-CDC50A Complex—ROS were purified by sucrose gradient centrifugation (27). The Rho-1D4, Atp6C11, and Cdc50–7F4 immunoaffinity columns were prepared as previously described (28). Purification of ATP8A2 was performed as described earlier (5). Briefly, 3.5 mg of ROS or a 10-cm dish of HEK293T cells were lysed in 1 ml of Buffer A for 30 min with stirring at 4 °C. Following solubilization, insoluble material was removed by centrifugation at 100,000 × *g* for 10 min. The detergent-solubilized fraction was added to ~30 μl of packed immunoaffinity matrix that had been pre-equilibrated in Buffer A. After a 2-h incubation, the matrix was washed six times with 500 μl of Buffer B and eluted twice for 30 min in 25 μl of Buffer B containing 0.2 mg/ml 1D4 or 6C11 peptides where appropriate. Protein was eluted from the Cdc50–7F4 column in Buffer B containing 2% SDS instead of 10 mM CHAPS. For reconstitution experiments, the columns were washed and eluted in Buffer C with the appropriate amount of peptide.

ATPase Activity Assay—ATPase activity was measured as described (5) at 37 °C for 15 min and stopped with 6% SDS. The amount of phosphate release was measured by the colorimetric method (29). Unless otherwise stated, ATP8A2 was assayed in the presence of 2.5 mg/ml lipid containing 100% PC, 10% PS, and 90% PC or 40% PE and 60% PC (w/w) in Buffer D with 5 mM ATP.

Reconstitution of ATP8A2-CDC50A Complex—Reconstitution was performed as described (5). Briefly, ~5 μg of purified ATP8A2-CDC50A in 150 μl of Buffer C was mixed 1:1 with Buffer E containing either 2.5% (w/w) NBD-PC, NBD-PE, or NBD-PS followed by dialysis overnight against 1 liter of Buffer F to remove the detergent.

Flippase Assay—Flippase assays were performed as described (5, 30, 31). Reconstituted ATP8A2 in 30 μl was mixed with either ATP or AMP-PNP to a final concentration of 0.5 mM with 50 μl of Buffer F and incubated at 23 °C for 2.5 min. Following incubation, 0.95 ml of Buffer F was added, and the sample was transferred to a cuvette (path length, 1 cm) and read in a fluorescence spectrophotometer (Varian, Palo Alto, CA) using excitation and emission wavelengths of 478 and 540 nm, respectively. After 2.5 min, sodium dithionite in 1 M Tris buffer, pH 10, was added to a final concentration of 2 mM. After 10 min, a stable base line was reached. Triton X-100 was added to final concentration of 1%, and the sample was read for an additional 1.5 min. The percentage of NBD lipid on the outside of the proteoliposomes was calculated using the following formula,

$$\%\mathrm{NBD}_{\mathrm{out}} = [(F_T - F_D)/(F_T - F_0)] \times 100 \qquad \text{(Eq. 1)}$$

where F_T is the total fluorescence of the sample before dithionite treatment, F_D is the fluorescence of the sample after dithionite treatment, and F_0 is the fluorescence after detergent solubilization. The percentage of flipped lipid was calculated from the difference between the transbilayer distribution of NBD lipids with ATP and AMP-PNP treatment.

Endoglycosidase Treatment of Rod Outer Segments—Approximately 50 μg of ROS were denatured at room temperature and subjected to PNGase F treatment at 37 °C for 1 h according to the manufacturer's instructions (New England Biolabs). The same amount of solubilized ROS in 10 mM CHAPS and 50 mM NaH_2PO_4, pH 5.0, was treated with neuraminidase (Roche Applied Science) for 1 h followed by *O*-glycosidase (Sigma) for 1 h according to the manufacturer's instructions.

Membrane Topology and Glycosylation Site Prediction—Membrane topology prediction was made using the TMHMM server, version 2.0 (32). Prediction of *N*-linked and *O*-linked

glycosylation was made using NetNGlyc 1.0 and NetOGlyc 3.1 servers, respectively (33, 34).

SDS-PAGE and Western Blots—The proteins were separated by SDS gel electrophoresis on 9% polyacrylamide gels and either stained with Coomassie Blue or transferred onto Immobilon FL membranes (Millipore, Bedford, MA) in buffer containing 25 mM Tris, pH 8.3, 192 mM glycine, 10% methanol. Immobilon membranes were blocked with 1% milk in PBS for 30 min; incubated with antibody supernatant typically diluted 1:100 for the Rho 1D4, 1:25 for Cdc50–9C9 and Atp6C11, and 1:10 for Cdc50–7F4 in PBS for 40 min; washed thoroughly with PBST (PBS containing 0.05% Tween 20); incubated for 40 min with secondary antibody, goat anti-mouse conjugated with IR dye 680, or IR dye 800 (LI-COR, Lincoln, NE) diluted 1:20,000 in PBST containing 0.5% milk; and washed with PBST prior to data collection on a LI-COR Odyssey infrared imaging system. The relative amounts of ATP8A2 were quantified on Western blots by LI-COR densitometry measurements and normalized to β-actin (Abcam, ab1801). Protein concentrations were estimated by Coomassie Blue staining of SDS-PAGE gels using known amounts of bovine serum albumin as a standard.

Tryptic Digestion and Mass Spectrometry—SDS-PAGE gels were divided into several equal slices and digested with trypsin according to established protocol (35). Peptides were concentrated using C_{18} stop and go extraction (STAGE) tips. The peptides were subjected to LC-MS/MS as described (22) using an LTQ-Orbitrap system (ThermoFisher, Bremen, Germany). The peptides were identified using the Mascot search program (36).

RESULTS

Identification of CDC50A as the β-Subunit for ATP8A2 by Mass Spectrometry—In previous studies, immunoaffinity-purified ATP8A2 from bovine ROSs was observed to migrate as a single 130-kDa protein on SDS gels stained with Coomassie Blue (5). However, a number of P_4-ATPases are known to associate with members of the Cdc50 protein family (14, 15, 18). Furthermore, CDC50A was identified as a protein present in photoreceptor outer segment preparations in a recent proteomic study (22). On this basis, we speculated that CDC50A may be associated with ATP8A2 but was undetectable in our purified ATP8A2 preparations by conventional protein staining techniques because of its highly glycosylated extracellular domain. To test this hypothesis, we digested immunoaffinity-purified ATP8A2 from photoreceptor membranes with trypsin for analysis by mass spectrometry. Tryptic peptides from both ATP8A2 and CDC50A were identified with a high level of confidence as shown in supplemental Table S2. Several proteins known to be highly abundant in outer segment preparations were also present including rhodopsin and tubulin. However, these proteins are commonly detected in immunoprecipitated protein samples from photoreceptor outer segments and therefore may represent residual contaminants in the preparation.

Monoclonal Antibodies to CDC50A—Because highly specific antibodies to CDC50A are not commercially available, we generated anti-Cdc50a monoclonal antibodies for use as probes to study the biochemical properties and localization of CDC50A and its interaction with ATP8A2. Two distinct monoclonal antibodies were obtained from mice immunized with GST fusion proteins comprising the N-terminal domain and part of the nonglycosylated portion of the exocytoplasmic domain of bovine CDC50A. One antibody designated as Cdc50–7F4 recognized the GST fusion protein comprising the N-terminal domain and another monoclonal antibody Cdc50–9C9 bound to the GST fusion protein containing part of the extracellular domain.

The specificity of these antibodies was confirmed on Western blots of CHAPS solubilized bovine ROS and HEK293T cells expressing 1D4 epitope-tagged bovine CDC50A (Fig. 1*A*). Both the Cdc50–7F4 and Cdc50–9C9 antibodies strongly labeled a 50-kDa protein in bovine ROS- and CDC50A-transfected HEK293T cells. The identity of the 50-kDa protein as CDC50A was further confirmed on Western blots of HEK293T cells expressing the 1D4-tagged CDC50A and labeled with the Rho-1D4 antibody. In addition to the 50-kDa protein, a 100-kDa protein was also observed in HEK293T cell extracts labeled with the Cdc50a and Rho 1D4 antibodies. This protein most likely represents a CDC50A dimer. CDC50A was not detected in HEK293T cells that had been mock transfected with empty plasmid. This further confirms the specificity of the monoclonal antibodies and further indicates that endogenous CDC50A expression in HEK293T cells is extremely low.

The anti-bovine Cdc50–7F4 antibody cross-reacted with the mouse and human orthologs, whereas the Cdc50–9C9 antibody was specific for the bovine protein (data not shown). Chemically synthesized peptides were used to map the epitope of the Cdc50–7F4 antibody to a 9-amino acid segment (AKDEVDGGP) encompassing positions 7–15 of bovine CDC50A. Finally, both CDC50A monoclonal antibodies did not label expressed CDC50B (data not shown).

Co-immunoprecipitation of ATP8A2 and CDC50A on Atp6C11 and Cdc50–7F4 Immunoaffinity Column—To confirm the association of ATP8A2 with CDC50A observed by mass spectrometry, ATP8A2 was purified from CHAPS solubilized ROS for analysis by Western blotting. Fig. 1*B* shows that the purified ATP8A2 ran as a 130-kDa protein as observed by Coomassie Blue staining and confirmed by Western blotting. The Cdc50–9C9 antibody intensely labeled the 50-kDa CDC50A protein, which was not visible in Coomassie Blue-stained gels. Essentially all of the CDC50A was associated with ATP8A2, because it was largely absent in the unbound fraction from the immunoaffinity column.

The ability of the Cdc50–7F4 antibody to immunoprecipitate the ATP8A2-CDC50A complex from ROS was investigated. As shown in Fig. 1*B*, the eluted fraction showed the 130-kDa Coomassie Blue-stained ATP8A2 protein and a small amount of contaminating antibody. Western blots labeled with the CDC50A and ATP8A2 specific antibodies confirmed the presence of both proteins in the elution fraction from the Cdc50–7F4 immunoaffinity support.

Expression and Localization of CDC50A in the Retina—The cellular and subcellular distribution of CDC50A and ATP8A2 in cryosections of bovine retina were compared by immunofluorescence microscopy. CDC50A labeling with the Cdc50–7F4 antibody was observed in the photoreceptor outer segments, as well as other retinal layers including a subset of ganglion cells

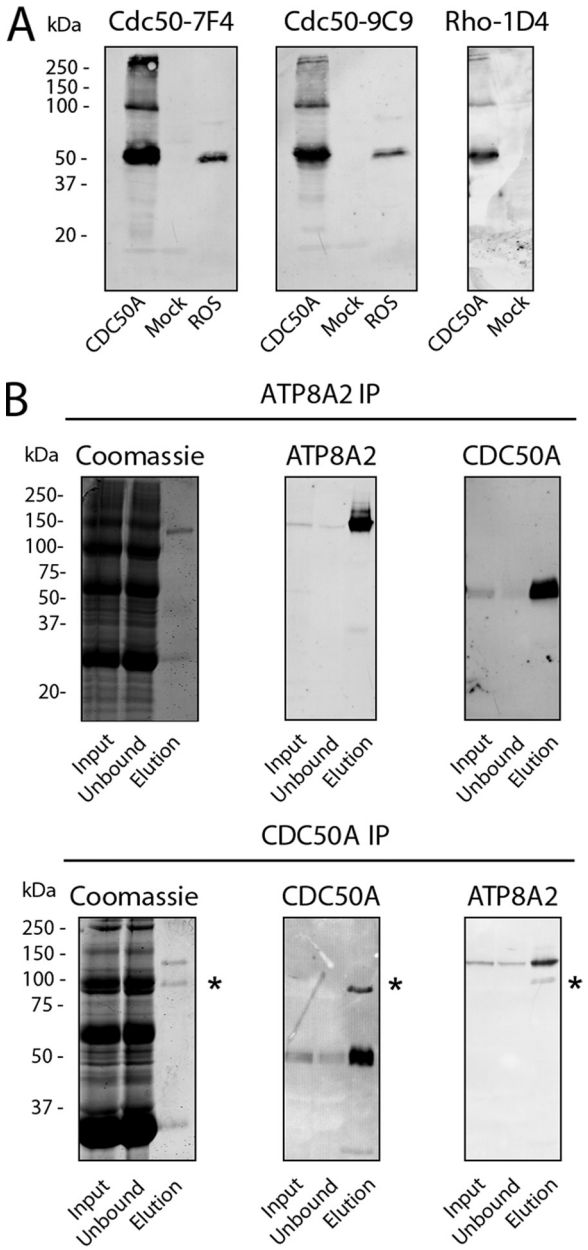

FIGURE 1. **CDC50A monoclonal antibodies and immunoprecipitation of the ATP8A2-CDC50A complex of rod outer segments.** *A*, Western blots of extracts from HEK293T cells transfected with *Cdc50a-1D4* plasmid (CDC50A) or empty plasmid (Mock) and bovine ROS membranes were labeled with monoclonal antibodies to CDC50A (Cdc50–7F4 and Cdc50–9C9) and Rho 1D4. *B*, Western blots of the ATP8A2-CDC50A complex immunoprecipitated (*IP*) from ROS membranes. CHAPS-solubilized ROS membranes (*Input*) were incubated with an immunoaffinity support consisting of either the ATP8A2 Atp6C11 antibody (*ATP8A2 IP*) or the CDC50A Cdc50–7F4 antibody (*CDC50A IP*) coupled to a Sepharose matrix. The fraction that did not bind to the column (*Unbound*) and the fraction that was eluted from the column (*Elution*) using either competing peptide 6C11 peptide (ATP8A2 IP) or 2% SDS (CDCC50A IP) were analyzed on SDS gels stained with Coomassie Blue and Western blots labeled with either the ATP8A2 or CDC50A specific antibodies. The *asterisks* indicate the presence of antibody present in the SDS-eluted fraction. Approximately 50 μg of input and unbound and 200 ng of elution were applied to the gel.

(Fig. 2*A*). In contrast, ATP8A2 labeling with the Atp2F6 antibody was restricted to the rod and cone outer segments as reported previously (5). No significant labeling of the Cdc50–7F4 antibody was observed in control samples treated with the competing 7F4 peptide. The presence of CDC50A in the retinal cell layers outside the photoreceptor outer segments suggests that CDC50A associates with other P_4-ATPases expressed in photoreceptors and other retinal cells.

To determine the gene expression profile of various members of the *Cdc50* family, RNA was extracted from retina and other tissues of 6-month-old C57/B6 mice for analysis by RT-PCR. A 600-bp fragment was amplified in all tissues using *cdc50a*-specific primers (Fig. 2*B*), confirming its ubiquitous tissue expression (37). High levels of expression of *cdc50a* were detected in the brain, retina, liver, lung, testis, and spleen with lower levels in the heart and kidney. Using *cdc50b* gene-specific primers, high mRNA levels were observed in the liver, kidney, lung, testis, and spleen but not the brain, retina, and heart (Fig. 2*B*). Finally, *cdc50c* expression was only seen in the testis, consistent with earlier reports indicating that *cdc50c* gene expression is restricted to spermatocytes and spermatids (38, 39). On the basis of these studies, *cdc50a* appears to be the only member of the *cdc50* family with detectable expression in adult mammalian retina.

The expression of the *cdc50* family in HEK293T cells, a human kidney cell line commonly used for overexpression of mammalian membrane proteins, was also investigated. *cdc50a* but not *cdc50b* or *cdc50c* expression was observed in this cell line as shown in supplemental Fig. S1.

ATP8A2 Expressed in HEK293T Cells Forms a Functional Complex with Endogenous CDC50A—Because HEK293T cells express low levels of CDC50A but not ATP8A2, we determined whether endogenous human CDC50A from HEK293T cells interacts with expressed ATP8A2 to form a functional complex. A detergent-solubilized extract from HEK293T cells expressing ATP8A2 was incubated with Atp6C11-Sepharose, and the bound protein was subsequently eluted with the competing 6C11 peptide. A relatively small amount of ATP8A2 was purified from these cells as visualized by Coomassie staining and Western blots (Fig. 3*A*). Western blots labeled with the Cdc50–7F4 antibody showed the presence of the endogenous 50-kDa CDC50A protein in the eluted fraction, which migrated as a broad band. Despite the low yield of purified ATP8A2, the ATPase activity of the protein complex was measured. The ATP8A2-CDC50A complex from HEK293T cells exhibited a high ATPase activity with PS, significantly lower levels with PE, and minimal activity in PC (Fig. 3*B*). The specific activity of 58 ± 1 μmol/min/mg for expressed ATP8A2 in the presence of PS was similar to the specific activity of 57 μmol/min/mg reported for the ATP8A2 complex isolated from bovine ROS (5).

Next, we investigated the effect of co-expression of CDC50A and ATP8A2 in HEK293T cells. In these studies, ATP8A2 was expressed without a tag, and CDC50A was expressed with a 1D4 tag to facilitate the identification and purification of the expressed complex. Significantly higher levels of ATP8A2 were obtained from cells co-expressing ATP8A2 and CDC50A (Fig. 3*C*). A 6-fold increase in ATP8A2 was observed for cells that had been co-transfected with *Atp8a2* and *Cdc50a* relative to cells transfected with only *Atp8a2* as determined after solubilization in SDS. Importantly, when membranes were solubilized

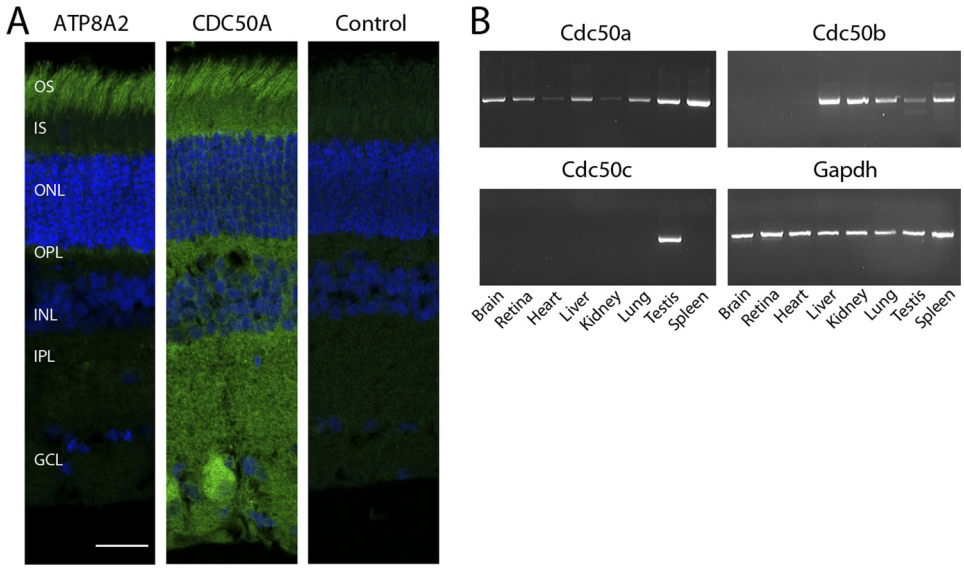

FIGURE 2. **Immunofluorescence localization of CDC50A in the retina and gene expression of CDC50 variants in the retina and other tissues.** *A*, retinal cryosections labeled with Atp2F6 or Cdc50–7F4 antibodies to ATP8A2 and CDC50A, respectively (*green*), and counterstained with the nuclear stain 4′,6-diamidino-2-phenylindole (*blue*). In the control sample, the CDC50A antibody was treated with excess 7F4 peptide prior to immunolabeling. CDC50A is abundantly localized in photoreceptor outer segments and other retinal layers. ATP8A2 is primarily restricted to the photoreceptor outer segment layer. *OS*, outer segments; *IS*, inner segments; *ONL*, outer nuclear layer; *OPL*, outer plexiform layer; *INL*, inner nuclear layer; *IPL*, inner plexiform layer; *GCL*, ganglion cell layer. *Bar*, 25 μm. *B*, gene expression of the *cdc50* family members in the retina and other tissues of adult mice by RT-PCR. *Gapdh* was used as a loading control. *Cdc50a* is the only member of the *cdc50* family detectable in the retina.

with the nondenaturing detergent CHAPS, a 15-fold increase in ATP8A2 was obtained from co-transfected cells.

ATPase and Lipid Flippase Activity of Expressed and Purified ATP8A2-CDC50A Complex—A dual immunoaffinity procedure was devised to study the functional activity of the ATP8A2-CDC50A complex from HEK293T cells co-expressing ATP8A2 and CDC50A with a 1D4 tag. A detergent-solubilized cell extract was first subjected to purification on an Atp6C11 immunoaffinity column. After elution with the competing 6C11 peptide, the complex was subjected to a second round of purification on a Rho-1D4 immunoaffinity column. This purification procedure has the potential of removing any free ATP8A2 or ATP8A2 associated with endogenous CDC50A.

Fig. 4*A* compares the purification of the ATP8A2-CDC50A complex on the Atp6C11 column with the complex isolated on the dual Atp6C11 and Rho 1D4 columns. A relatively high yield of the ATP8A2-CDC50A complex was obtained by either procedure as visualized in the Coomassie Blue-stained eluted fractions (Fig. 4*A*). Western blots indicated that the CDC50A-1D4 protein co-purified with ATP8A2 and ran as a broad band. In a typical experiment, the expressed complex purified only on an Atp6C11 immunoaffinity matrix resulted in a specific activity of 67 $\pm$ 2 μmol/min/mg, and the complex isolated on the Atp6C11 and Rho1D4 matrix resulted in a slightly higher specific activity of 76 $\pm$ 3 μmol/min/mg (Fig. 4*B*). The small increase in activity found after the dual immunoaffinity purification procedure most likely results from the removal of residual nonfunctional forms of ATP8A2 not associated with CDC50A-1D4.

The aminophospholipid flippase activity of the ATP8A2-CDC50A complex expressed in HEK293T cells and isolated by the dual immunoaffinity procedure was measured using the fluorescence-based NBD-labeled lipid assay (30, 31). The purified complex reconstituted into liposomes containing NBD-labeled lipid was incubated with ATP or the nonhydrolyzable ATP analog, AMP-PNP as a control. Dithionite was then added to bleach the NBD lipids on the outer surface of the liposomes, resulting in a decrease in the fluorescence signal. The extent of lipid transport or flipping was determined from the difference in fluorescence observed with ATP *versus* AMP-PNP after dithionite treatment.

A typical fluorescence trace for liposomes reconstituted with ATP8A2-CDC50A and containing NBD-labeled PS is shown in supplemental Fig. S2*A*. Liposomes incubated with ATP showed a 6% decrease in fluorescence relative to liposomes incubated with AMP-PNP after treatment with dithionite. This reflects ATP8A2-CDC50A-mediated ATP-dependent transport of NBD-labeled PS from the inner to the outer leaflet of the liposomes. In control experiments, vesicles lacking ATP8A2-CDC50A showed no difference in fluorescence signal with ATP or AMP-PNP after the addition of dithionite (supplemental Fig. S2*B*).

The flippase activity of the purified and reconstituted ATP8A2-CDC50A complex from co-transfected HEK293T cells was measured for various aminophospholipid substrates (Fig. 4*C*). The complex transported up to 6% of the total NBD-labeled PS, but only 1% of the NBD-labeled PE, and essentially no NBD-labeled PC. In an earlier study, no transport of NBD-PE was observed for ATP8A2 complex purified from ROS (5). This was likely due to the lower amounts of protein present in the reconstituted vesicles. As expected, the PS flippase activity of ATP8A2-CDC50A was found to be dependent on the amount of protein reconstituted into the liposomes (Fig. 4*C*).

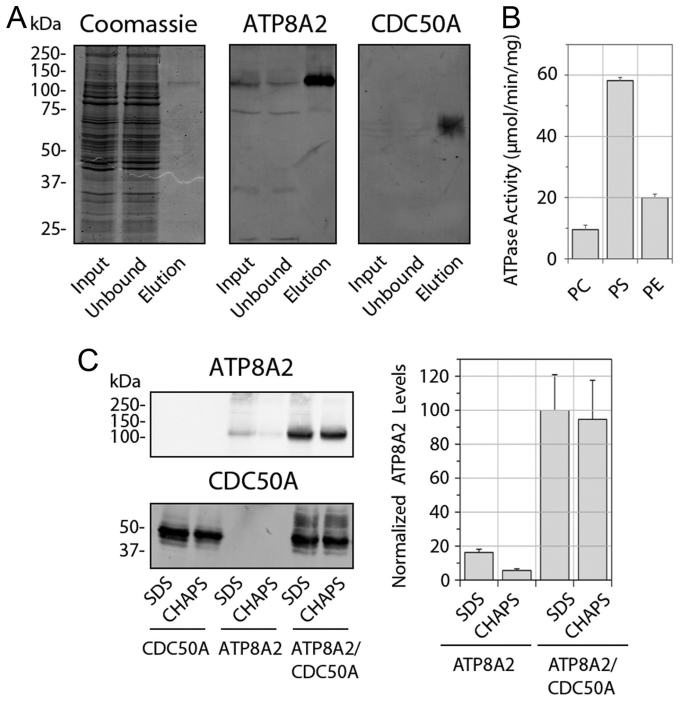

FIGURE 3. **ATP8A2 expressed in HEK293T cells interacts with endogenous CDC50A to form a catalytically active ATP8A2-CDC50A complex.** *A*, immunoaffinity purification of ATP8A2-CDC50A complex from HEK293T cells transfected with the *Atp8A2* plasmid. Solubilized HEK293T cell extract (*Input*) was incubated with the Atp6C11 immunoaffinity matrix, and the unbound fraction (*Unbound*) and the 6C11 peptide eluted fraction (*Elution*) were analyzed on SDS gels stained with Coomassie Blue, and Western blots were labeled with the Atp6C11 antibody (*ATP8A2*) and the Cdc50–7F4 antibody (*CDC50A*). *B*, ATPase activity of the purified ATP8A2-CDC50A complex in 100% phosphatidylcholine (*PC*) or 10% phosphatidylserine (*PS*) or 40% phosphatidylethanolamine (*PE*) each containing the corresponding concentrations of PC. *C*, quantitative analysis of expressed and solubilized ATP8A2 and CDC50A. ATP8A2 and CDC50A containing a 1D4 tag were expressed individually (*ATP8A2* or *CDC50A*) or together (*ATP8A2/CDC50A*) in HEK293T cells. The amounts of ATP8A2 and CDC50A solubilized with either SDS or CHAPS were measured by Western blotting (*left*), and the relative quantity of solubilized ATP8A2 was determined from Western blots of three experiments (*right*). Approximately, 30 μg of protein was loaded into each lane.

Expression, Co-immunoprecipitation and Functional Characterization of CDC50A/CDC50B Chimera Proteins—The CDC50B variant is 55% identical to CDC50A and displays a similar membrane topology (Fig. 5*A*). However, as previously reported (19) and confirmed in this study (Fig. 5*B*), CDC50B, unlike CDC50A, does not interact with ATP8A2. We have taken advantage of this property to begin to define regions of CDC50A that are required for the formation of a functionally active ATP8A2-CDC50A complex. Chimera proteins consisting of a combination of CDC50A and CDC50B domains (Fig. 5*A*) were constructed and co-expressed with ATP8A2 in HEK293T cells. The interaction of ATP8A2 with the CDC50 chimera proteins was determined by co-immunoprecipitation of these proteins on an anti-ATP8A2 immunoaffinity matrix. As shown in Fig. 5*B*, CDC50 chimera proteins in which either the ECD or the N-terminal domain of CDC50B was replaced with corresponding domain of CDC50A failed to interact with ATP8A2. In contrast, the CDC50 chimera protein in which the exocytoplasmic domain and the transmembrane domain consisting of both M1 and M2 (ECD/TM) of CBC50B were replaced with the corresponding CDC50A domains expressed at relatively high levels and co-immunoprecipitated with the ATP8A2. A chimera protein containing the exocytoplasmic domain, the transmembrane domain, and the C-terminal domain (ECD/TM/C) of CDC50A also interacted with ATP8A2. However, chimera proteins in which one or both transmembrane segments (M1/M2) of CDC50B were replaced with the transmembrane segments of CDC50A failed to interact with ATP8A2 (supplemental Fig. S3).

The PS-dependent ATPase activities of the purified ATP8A2-CDC50 chimera protein complexes were studied. As shown in Fig. 5*C*, the ECD/TM and ECD/TM/C chimera protein complexes displayed substantially lower PS-dependent ATPase activities compared with the WT ATP8A2-CDC50A complex. The WT ATP8A2-CDC50A complex had a V_{max} of 107 ± 8 μmol/min/mg, whereas the ATP8A2-ECD/TM and ATP8A2-ECD/TM/C complexes had V_{max} of 40 ± 5 and 35 ± 5 μmol/min/mg, respectively. The K_m values of the ECD/TM and ECD/TM/C chimera complexes (K_m of 86 ± 35 and 73 ± 32 μM, respectively), however, were similar to the WT protein (K_m of 98 ± 24 μM).

Vanadate is known to be a potent inhibitor of P-type ATPases and is often used to measure changes in the equilibrium between the E1 and E2 conformational states of ATPases during the reaction cycle. Fig. 5*C* shows that the ATPase activity of purified WT ATP8A2-CDC50A complex is strongly inhibited by vanadate with K_i of 2.7 ± 0.3 μM. The chimera complexes showed a decrease in sensitivity to vanadate exhibiting a K_i for the ECD/TM and ECD/TM/C chimera complexes of 8.7 ± 0.8 and 7.3 ± 0.7 μM, respectively.

The aminophospholipid flippase activity of equal amounts of purified and reconstituted ATP8A2-CDC50 chimeras was studied (Fig. 5*D*). The WT complex was able to transport 6.7 ± 0.3% of total NBD-PS. In contrast, the chimeras were able to transport less NBD-PS consistent with the PS-dependent ATPase studies. The ECD/TM and ECD/TM/C chimeras transported 3.5 ± 0.4 and 4.2 ± 0.5%, respectively.

Localization of ATP8A2-CDC50 Complexes in Transfected Cos-7 Cells—The subcellular distribution of ATP8A2 and CDC50A individually and co-expressed in Cos-7 cells was investigated in double labeling studies using calnexin as an ER marker and GM130 as a Golgi marker. For these studies, ATP8A2 and CDC50A contained C-terminal 1D4 and Myc tags, respectively, to facilitate double labeling. Immunoprecipitation studies and ATPase assays indicated that the C-terminal tags had no effect on the interaction of ATP8A2 with CDC50A or functional activity of the complex. The majority of ATP8A2 and CDC50A co-localized with calnexin in the ER in singly transfected cells (supplemental Fig. S4). In contrast, ATP8A2 and CDC50A co-localized with GM130 in the Golgi of co-transfected cells. This indicates that the association of ATP8A2 with CDC50A resulted in the translocation of the complex from the ER to the Golgi. A similar distribution pattern has been recently reported in cultured U20S cells expressing ATP8A2 and CDC50A (19), indicating that this distribution is not specific to Cos-7 cells.

The effect of CDC50 chimera proteins on the localization of ATP8A2 was investigated. When ATP8A2 was co-expressed with the noninteracting CDC50 chimera proteins, ECD or

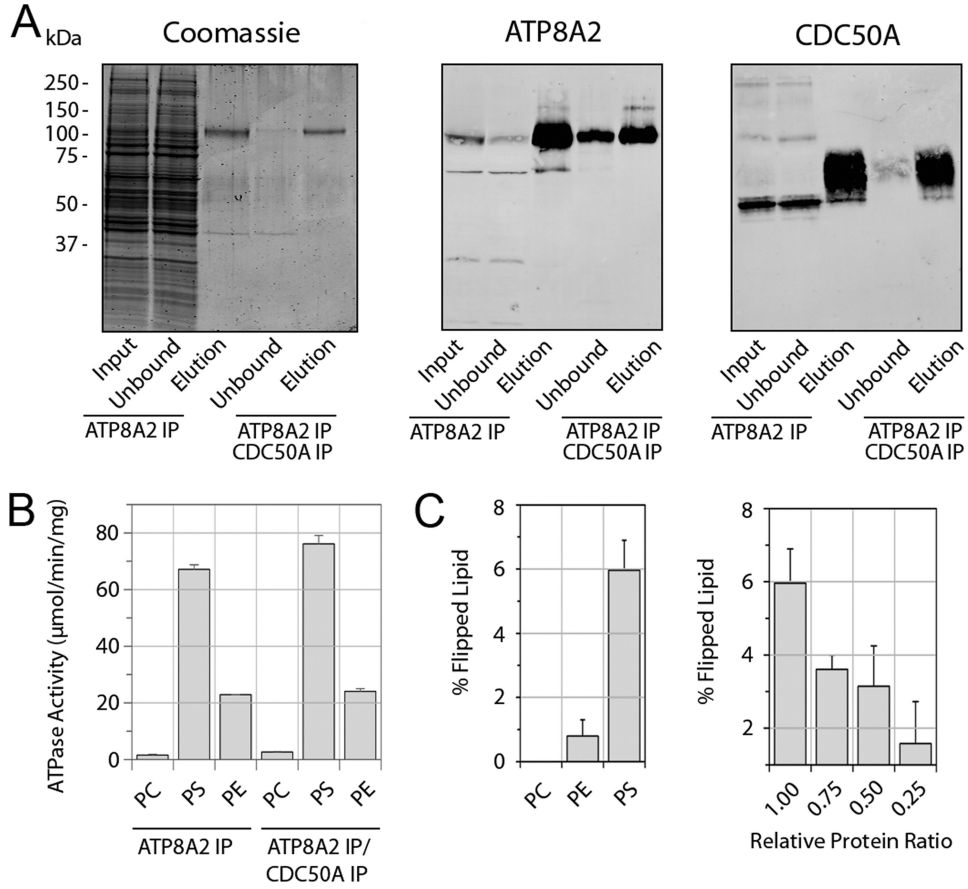

FIGURE 4. **ATPase activity and phospholipid flippase activity of the expressed and purified ATP8A2-CDC50A complex.** *A*, Coomassie Blue-stained gel and Western blots of the immunoaffinity-purified ATP8A2-CDC50A complex from HEK293T cells co-expressing both ATP8A2 and CDC50A-1D4. The complex was purified on either an Atp6C11 column alone (*ATP8A2 IP*) or sequentially on Atp6C11 and Rho-1D4 columns (*ATP8A2/CDC50A IP*). *B*, ATP8A2 and CDC50A containing a 1D4 tag were co-expressed in HEK293T cells, and the complex was purified by the dual immunoaffinity procedure. The ATPase activity of the complex was measured in the presence of 100% PC or 10% PS or 40% PE lipids each containing the appropriate amount of PC. *C*, the ATP8A2-CDC50A complex purified by the dual immunoaffinity procedure was reconstituted into liposomes for phospholipid flippase measurements. The percentage of lipid flipped by the ATP8A2-CDC50A complex was measured in phosphatidylcholine proteoliposomes for 2.5% NBD-labeled PC, PE, or PS. *Right panel*, the PS flippase activity of the ATP8A2-CDC50A complex was measured for decreasing amounts of reconstituted protein. *IP*, immunoprecipitation.

N-terminal domain, ATP8A2 co-localized with calnexin in ER similar to that observed with noninteracting CDC50B (Fig. 6). However, when ATP8A2 was co-expressed with the ECD/TM or ECD/TM/C chimera proteins, it co-localized with GM130 to the Golgi similar to that observed for the WT ATP8A2-CDC50A complex. These results suggest that the ECD/TM and ECD/TM/C chimera proteins promote the folding of ATP8A2 into a native-like conformation, allowing the complex to exit the ER and translocate to the Golgi.

N-Linked Glycosylation of CDC50A Is Required for the Stable Expression of ATP8A2—The exocytoplasmic domain of CDC50A contains four consensus sequences for *N*-linked glycosylation and one possible site for *O*-linked glycosylation. To determine whether endogenous bovine CDC50A is glycosylated, detergent-solubilized ROS membranes were treated with enzymes known to remove oligosaccharide chains from glycoproteins and analyzed on Western blots labeled with the Cdc50–9C9 antibody. Treatment with PNGase F, which removes *N*-linked sugars, resulted in a marked decrease in the apparent molecular mass from 50 to 37 kDa close to the predicted molecular mass of the CDC50A polypeptide (Fig. 7*A*). In contrast, no detectable shift in molecular mass was observed after treatment with neuraminidase alone or in combination with *O*-glycosidase.

The effect of *N*-glycosylation of CDC50A on the expression and interaction with ATP8A2 was studied with mutants in which single and multiple consensus sequences for *N*-glycosylation were abolished. Co-expression of single *N*-glycosylation defective mutants of CDC50A (T109A, T182A, S192A, and T296A) with ATP8A2 showed a reduction in ATP8A2 expression levels relative to co-expression with WT CDC50A (Fig. 7*B*). In contrast, the mutation that abolished the putative *O*-linked glycosylation (T285A) showed no reduction in ATP8A2 expression.

Multiple glycosylation site mutants Δ2 (T109A,T182A), Δ3 (T109A,T182A,S192A), and Δ4 (T109A,T182A,S192A,T296A) showed an inverse additive effect on the ATP8A2 expression levels (Fig. 7*B*). The CDC50A Δ2 mutant resulted in a 60% reduction in ATP8A2 expression relative to WT CDC50A, whereas the Δ3 mutant showed an 80% reduction, and the Δ4 mutant reduced ATP8A2 expression to levels that were essentially undetectable in cell lysates.

Co-immunoprecipitation studies were carried out to determine whether the *N*-glycosylation mutants interact with

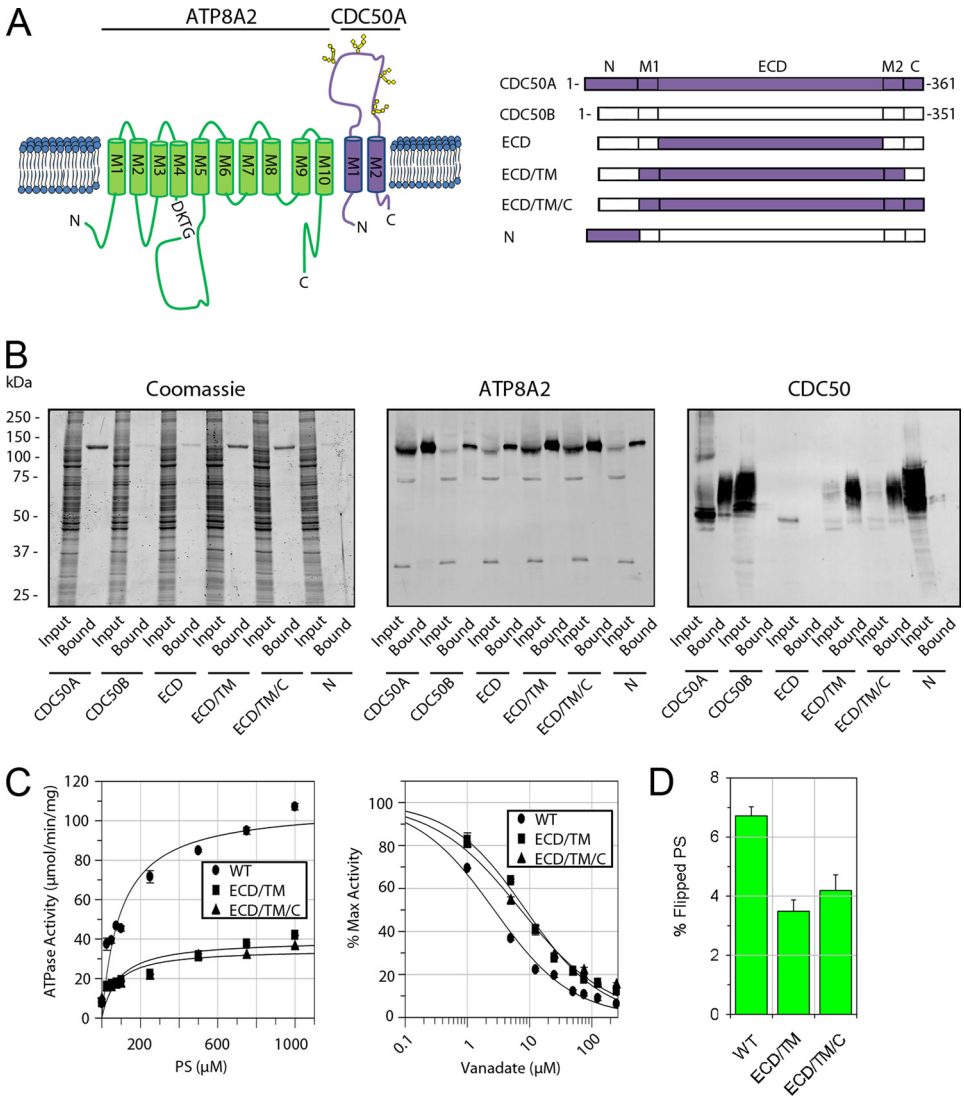

FIGURE 5. **Interaction and functional activity of ATP8A2-CDC50 complexes containing CDC50A/B chimera proteins.** *A*, topological model of the ATP8A2-CDC50A complex (*left panel*). ATP8A2 is shown in *green*, and CDC50A is in *purple*. The phosphorylated motif (*DKTG*) is indicated along with the positions of the *N*-linked glycosylation sites on CDC50A. *Right panel*, schematic showing various chimera CDC50A/B proteins used in these studies. *B*, interaction of CDC50A/B chimera proteins containing a 1D4 tag with ATP8A2. Proteins were purified on an ATP8A2 immunoaffinity column and analyzed on SDS gels stained with Coomassie Blue or Western blots labeled with an ATP8A2 antibody (*ATP8A2*) or Rho-1D4 antibody (*CDC50*). CDC50A co-purified with ATP8A2, whereas CDC50B did not. Chimera proteins containing only the extracellular domain (*ECD*) or N-terminal domain (*N*) of CDC50A did not co-purify with ATP8A2. Chimeras containing the ECD and TM domain consisting of both M1 and M2 segments (*ECD/TM*) or the ECD, TM, and C-terminal domains (*ECD/TM/C*) of CDC50A co-purified with ATP8A2. *C*, *left panel*, ATPase activity of ATP8A2 associated with either WT CDC50A (*WT*) or chimera CDC50A proteins (ECD/TM or ECD/TM/C) as a function of PS concentration in the presence of PC. *Right panel*, vanadate inhibition of ATPase activity of ATP8A2-CDC50 complexes in 1000 μM PS in the presence of PC. *D*, flippase activity of ATP8A2-CDC50 complexes containing WT CDC50A and the ECD/TM and ECD/TM/C chimeras reconstituted in phosphatidylcholine in the presence of 2.5% NBD-PS.

ATP8A2. As shown in Fig. 7*C*, all of the single CDC50A glycosylation mutants co-precipitated with ATP8A2. Western blots of the WT and mutant CDC50A proteins prior to immunoprecipitation (input) showed an intense compact 50-kDa protein band and a faint diffuse slower migrating band. After immunoprecipitation of ATP8A2, only the slower diffuse migrating band corresponding to the heterogeneous glycosylated form of CDC50A was present in the bound and eluted fraction. An exception was the S192A CDC50A mutant, which ran as a relatively sharp, intense band migrating just above the 50-kDa band along with a small amount of a slower migrating diffuse band. This suggests that most of the single *N*-glycosylation mutants interact with ATP8A2 and undergo heterogeneous glycosylation similar to that observed for WT CDC50A.

Next, we assessed whether the multiple *N*-glycosylation CDC50A mutants interact with ATP8A2. Fig. 7*D* shows that multiple *N*-glycosylation mutants (Δ2, Δ3, and Δ4) co-precipitated with ATP8A2. The mutants migrated as sharp multiple bands of decreasing molecular weights with the Δ4 mutant having a molecular mass comparable with that observed for WT CDC50A treated with PNGase F. Finally, we subjected the glycosylation mutant ATP8A2-CDC50A complexes to the double immunoaffinity purification to remove any endogenous WT CDC50A bound to ATP8A2 and tested the eluted complexes for PS-dependent ATPase activity. All of the mutants with the exception of T296A, Δ3, and Δ4 were isolated in sufficient quantity for analysis. Each mutant complex exhibited specific ATPase activities comparable with the WT complex (Fig. 7*E*).

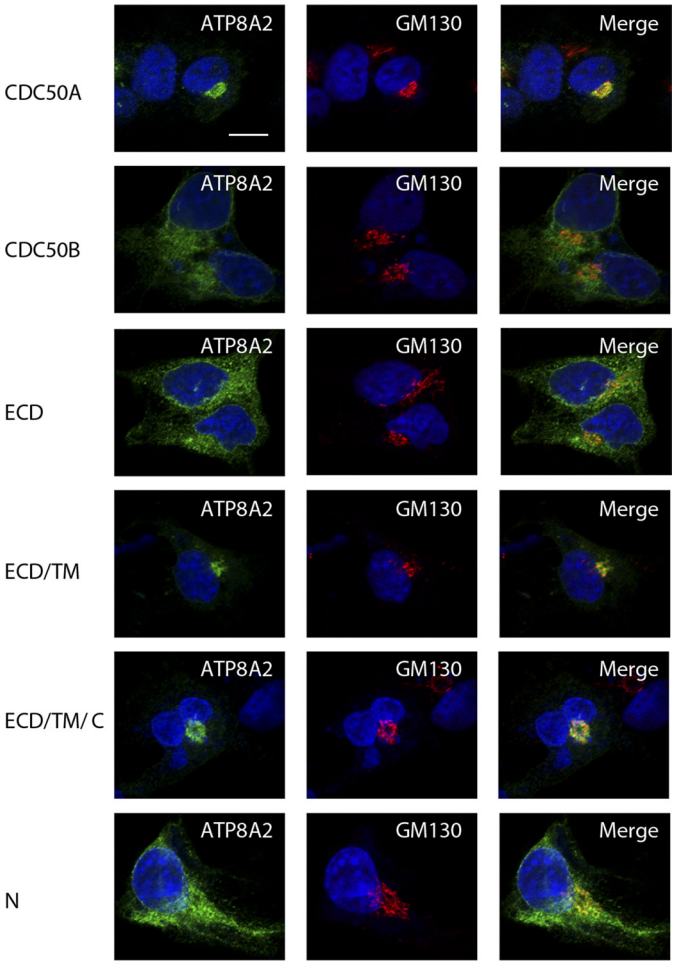

FIGURE 6. **Immunofluorescence localization of ATP8A2 co-expressed with WT CDC50A, WT CDC50B, or chimera CDC50A/B containing a 1D4 tag in Cos-7 cells.** The cells were double labeled for ATP8A2 with the Atp2F6 monoclonal antibody (*green*) and the *GM130* polyclonal antibody as a Golgi marker (*red*). Co-expression of ATP8A2 with CDC50B or chimeric CDC50A proteins containing the *ECD* or N-terminal domain (*N*) domains resulted in a reticular staining pattern of ATP8A2 characteristic of ER localization. Co-expression of ATP8A2 with either WT CDC50A or chimera proteins containing the *ECD/TM* or *ECD/TM/C* domains of CDC50A resulted in localization of ATP8A2 to the Golgi as shown in merged images. Expression of CDC50 proteins was confirmed independently using the Rho 1D4 antibody (data not shown). The nuclei (*blue*) were labeled with 4′,6-diamidino-2-phenylindole. *Bar*, 10 μm.

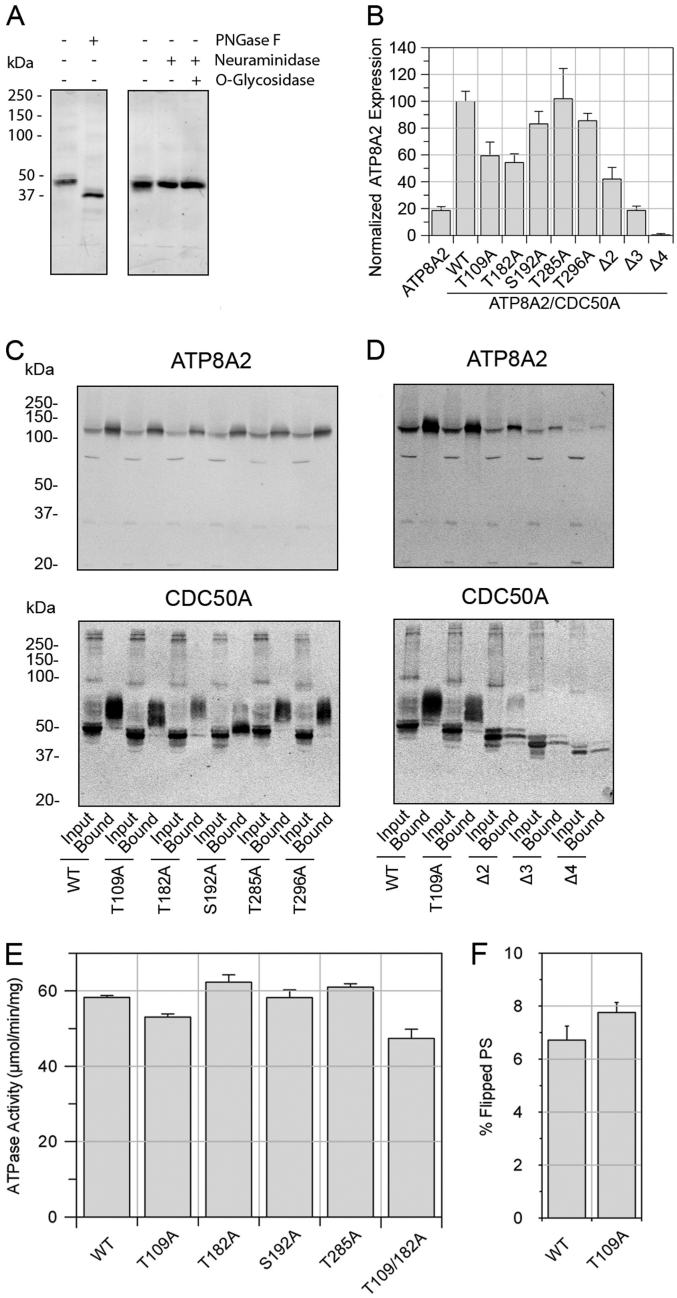

FIGURE 7. ***N*-Linked glycosylation of CDC50A is necessary for stabilization of ATP8A2.** *A*, approximately 50 μg of rod outer segment membranes were treated with PNGase F or neuraminidase with or without *O*-glycosidase and labeled with the Cdc50–9C9 antibody. *B*, expression levels of ATP8A2 in the presence of CDC50A glycosylation mutants containing a 1D4 tag. ATP8A2 levels were normalized to β-actin as a loading control. *C*, co-immunoprecipitation of single CDC50A glycosylation mutants with ATP8A2 on Atp6C11-Sepharose. ATP8A2 was detected with Atp6C11, and the CDC50A-1D4 mutants were detected with the Rho 1D4 antibody. Solubilized HEK293T cells (*Input*) were incubated in the column, and the bound proteins (*Bound*) were eluted with 6C11 peptide. *D*, immunoprecipitation of multiple CDC50A glycosylation mutants with ATP8A2 on Atp6C11-Sepharose. Multiple site CDC50A glycosylation mutants expressed at low levels relative to WT CDC50A. Approximately 30 μg of input and 5–200 ng of the bound fractions were applied to the gel. *E*, specific ATPase activity of ATP8A2 expressed with various CDC50A *N*-linked glycosylation mutants and purified on an immunoaffinity column. ATPase activity was measured in the presence of 10% PS and 90% PC. *F*, lipid flippase activity of WT and T109A mutant reconstituted in PC in the presence of 2.5% NBD-PS. The difference in activities between WT and T109A is not significant.

The flippase activity for the T109A glycosylation mutants was also found to be similar to WT (Fig. 7*F*).

DISCUSSION

Although the interaction of P_4-ATPases with CDC50 proteins has been observed in cells co-expressing these proteins, the association of endogenous CDC50 proteins with endogenous P_4-ATPases in animal cells has not been reported to date. In the present study, we show that ATP8A2 purified from photoreceptor outer segment membranes exists as a heteromeric complex with CDC50A by both mass spectrometry and Western blotting. The purified and reconstituted complex functions as a PS and to a lesser degree PE lipid transporter as previously reported (5). Immunofluorescence labeling studies using the highly specific ATP8A2 monoclonal antibody Atp2F6 and the CDC50A monoclonal antibody Cdc50–7F4 generated as part

of this study show that these proteins co-localize to the outer segment compartment of photoreceptor cells. Although ATP8A2 is restricted to the outer segments, CDC50A is also present in other retinal cells and other cellular compartments of photoreceptor cells. This suggests that CDC50A also forms a heteromeric complex with other P_4-ATPases in the retina. It should be possible to use the CDC50A specific monoclonal antibodies in conjunction with immunoprecipitation and mass spectrometry to identify and characterize the various P_4-ATPases in the retina and other tissues.

In a recent study, ATP8A2 and other class 1 P_4-ATPases were found to associate with CDC50 variants when co-expressed in U2OS cells and promote the export of these complexes from the ER (19). However, the function of these complexes as phospholipid-dependent ATPases or ATP-dependent lipid transporters was not determined. Here, we have confirmed that ATP8A2 forms a heteromeric complex with CDC50A, but not CDC50B, in HEK293T and Cos-7 cells, and this complex is translocated from the ER to the Golgi. Importantly, we show for the first time that this expressed complex is functionally active as an aminophospholipid transporter when reconstituted into lipid vesicles.

HEK293T cells express low levels of endogeneous CDC50A. When cells are transfected with *Atp8a2* alone, a small fraction of the heterologously expressed ATP8A2 interacts with endogenous CDC50A. Although the yield of this ATP8A2-CDC50A complex is low, nonetheless it shows PS- and PE-dependent ATPase activity similar to that previously observed for ATP8A2-CDC50A complex isolated from photoreceptor outer segments (5). The low quantity of the complex is likely due to the limiting expression of endogenous CDC50A in HEK293T cells because co-expression of ATP8A2 with CDC50A greatly enhances the yield of functionally active complex.

The role of CDC50A in promoting a stable active complex is supported by immunolabeling studies of ATP8A2 and CDC50A expressed in Cos-7 cells. In the absence of expressed CDC50A, the majority of the expressed ATP8A2 is retained in the ER, most likely as a misfolded protein that is poorly soluble in mild detergent. Co-expression of ATP8A2 with CDC50A results in the formation of properly folded heteromeric complex that is transported from the ER and to the Golgi compartment and is readily solubilized in CHAPS detergent as a functionally active PS-dependent ATPase.

CDC50A does not appear to direct the subcellular targeting of P_4-ATPases. It has been previously reported that ATP8B1 associated with CDC50A localizes to the plasma membrane of culture cells (15), whereas ATP8A2 associated with CDC50A localizes to the Golgi compartment. Hence, the cell targeting signals of most, if not all, mammalian P_4-ATPases appear to reside in the catalytic P_4-ATPase subunit. This is in agreement with studies of Lopez-Marques *et al.* (18), who showed that *Arabidopsis* P_4-ATPases ALA2 and ALA3 and not CDC50 proteins are responsible for subcellular targeting of the complex.

In HEK293T cells, CDC50A expressed by itself is retained in the ER. It migrates as a relatively compact 50-kDa protein on SDS gels. In contrast, CDC50A associated with ATP8A2 and is present in the Golgi migrates as a diffuse band. This suggests that the *N*-linked oligosaccharide chains of CDC50A undergo extensive heterogeneous modification within the Golgi of HEK293T cells. This highly heterogeneous glycosylation appears to be a characteristic of ATP8A2-CDC50A overexpression in culture cells because CDC50A associated with ATP8A2 in photoreceptor outer segments migrates as a more compact band. A similar difference in migration pattern has been reported for the *N*-linked glycoprotein rhodopsin. Rhodopsin from rod outer segments migrates as a relatively tight band on SDS gels, whereas rhodopsin expressed in culture cells migrates as a diffuse band characteristic of heterogeneous *N*-linked glycosylation (40). This pattern most likely reflects a difference in the processing of oligosaccharide chains in these distinct cell types.

The four highly conserved *N*-linked glycosylation consensus sequences in the exocytoplasmic domain of CDC50A all undergo glycosylation. Analysis of single and multiple glycosylation mutants indicate that each oligosaccharide chain contributes to the optimal, stable expression of the ATP8A2-CDC50A complex. Although the loss of one or more glycosylation sites reduces the yield of the complex, it does not appear to affect the functional activity of the ATP8A2-CDC50A complex as measured by PS-stimulated ATPase and flippase assays.

In this study chimera CDC50A/B proteins were generated and used to investigate the role of the various domains of CDC50A in the binding and functional activity of ATP8A2. Chimera proteins in which either the TM or the ECD domain of CDC50B was replaced with the corresponding CDC50A domain on a CDC50B backbone failed to interact with ATP8A2. In contrast, the chimera protein with both domains (ECD/TM) replaced assembled with ATP8A2 into a functionally active complex capable of actively transporting PS across the lipid bilayer. Like the WT protein complex, this chimera complex was also exported from the ER to the Golgi. This indicates that both ECD and TM domains of CDC50A are required for the proper folding, subunit assembly, and function of the ATP8A2-CDC50 complex as a PS flippase. A similar situation exists for the Na/K-ATPase. Both the transmembrane and extracellular domains of the β-subunit of Na/K-ATPase have been implicated in its interaction with the catalytic α-subunit and contribute to the transport mechanism (41–43).

The ECD/TM/C chimera protein containing the C-terminal as well as the ECD and TM domains of CDC50A exhibited similar properties as the ECD/TM chimera. This indicates either that the C terminus is not involved in the interaction with ATP8A2 or that the C-terminal domain of CDC50B can effectively substitute for the C-terminal domain of CDC50A in this capacity. Interestingly, although the ECD/TM and ECD/TM/C chimera interact with ATP8A2 to form a functional complex, the PS-dependent ATPase activity and lipid flippase activity are significantly reduced. Likewise, these chimeric complexes have a decreased sensitivity to vanadate, a P-type ATPase inhibitor that interacts with the E2 state. Collectively, these studies suggest that the N-terminal domain plays a role in the transport cycle of ATP8A2. One possibility is that CDC50A plays a similar role as the β-subunit of the H^+/K^+ ATPase stabilizing the E2P state of the enzyme through its N-terminal domain (44). Our finding that CDC50A participates in the ATPase reaction

cycle of ATP8A2 is in general agreement with recent studies on the yeast Drs2p-Cdc50p and the ATP8B1-CDC50 P_4-ATPases (20, 21).

In summary, our studies show that CDC50A is the β-subunit of ATP8A2 in photoreceptor outer segment membranes and is essential for the proper folding, assembly, and exit of the ATP8A2-CDC50A complex from the ER to the Golgi in culture cells. Importantly, CDC50A is also critical for the formation of a functionally active complex that can catalyze the transport of PS and to a lesser extent PE across cell membranes. Both the transmembrane and exocytoplasmic domains of CDC50A are essential for the formation of a functionally active ATP8A2-CDC50A complex, whereas the N-terminal domain of CDC50A participates in the reaction cycle of ATP8A2, possibly stabilizing the E2P state. Finally, *N*-linked glycosylation of CDC50A plays an important role in the formation of a stable ATP8A2-CDC50A protein complex.

Acknowledgments—We thank Laurie Molday and Theresa Hii for technical assistance in the generation and maintenance of hybridoma cell lines.

REFERENCES

1. Alder-Baerens, N., Lisman, Q., Luong, L., Pomorski, T., and Holthuis, J. C. (2006) *Mol. Biol. Cell* **17,** 1632–1642
2. Darland-Ransom, M., Wang, X., Sun, C. L., Mapes, J., Gengyo-Ando, K., Mitani, S., and Xue, D. (2008) *Science* **320,** 528–531
3. Natarajan, P., Wang, J., Hua, Z., and Graham, T. R. (2004) *Proc. Natl. Acad. Sci. U.S.A.* **101,** 10614–10619
4. Wang, L., Beserra, C., and Garbers, D. L. (2004) *Dev. Biol.* **267,** 203–215
5. Coleman, J. A., Kwok, M. C., and Molday, R. S. (2009) *J. Biol. Chem.* **284,** 32670–32679
6. Zhou, X., and Graham, T. R. (2009) *Proc. Natl. Acad. Sci. U.S.A.* **106,** 16586–16591
7. Folmer, D. E., Elferink, R. P., and Paulusma, C. C. (2009) *Biochim. Biophys. Acta* **1791,** 628–635
8. Muthusamy, B. P., Natarajan, P., Zhou, X., and Graham, T. R. (2009) *Biochim. Biophys. Acta* **1791,** 612–619
9. Puts, C. F., and Holthuis, J. C. (2009) *Biochim. Biophys. Acta* **1791,** 603–611
10. Bull, L. N., van Eijk, M. J., Pawlikowska, L., DeYoung, J. A., Juijn, J. A., Liao, M., Klomp, L. W., Lomri, N., Berger, R., Scharschmidt, B. F., Knisely, A. S., Houwen, R. H., and Freimer, N. B. (1998) *Nat. Genet.* **18,** 219–224
11. Meguro, M., Kashiwagi, A., Mitsuya, K., Nakao, M., Kondo, I., Saitoh, S., and Oshimura, M. (2001) *Nat. Genet.* **28,** 19–20
12. Stapelbroek, J. M., Peters, T. A., van Beurden, D. H., Curfs, J. H., Joosten, A., Beynon, A. J., van Leeuwen, B. M., van der Velden, L. M., Bull, L., Oude Elferink, R. P., van Zanten, B. A., Klomp, L. W., and Houwen, R. H. (2009) *Proc. Natl. Acad. Sci. U.S.A.* **106,** 9709–9714
13. Cacciagli, P., Haddad, M. R., Mignon-Ravix, C., El-Waly, B., Moncla, A., Missirian, C., Chabrol, B., and Villard, L. (2010) *Eur. J. Hum. Genet.* **18,** 1360–1363
14. Saito, K., Fujimura-Kamada, K., Furuta, N., Kato, U., Umeda, M., and Tanaka, K. (2004) *Mol. Biol. Cell* **15,** 3418–3432
15. Paulusma, C. C., Folmer, D. E., Ho-Mok, K. S., de Waart, D. R., Hilarius, P. M., Verhoeven, A. J., and Oude Elferink, R. P. (2008) *Hepatology* **47,** 268–278
16. Poulsen, L. R., López-Marqués, R. L., McDowell, S. C., Okkeri, J., Licht, D., Schulz, A., Pomorski, T., Harper, J. F., and Palmgren, M. G. (2008) *Plant Cell* **20,** 658–676
17. Chen, S., Wang, J., Muthusamy, B. P., Liu, K., Zare, S., Andersen, R. J., and Graham, T. R. (2006) *Traffic* **7,** 1503–1517
18. López-Marqués, R. L., Poulsen, L. R., Hanisch, S., Meffert, K., Buch-Pedersen, M. J., Jakobsen, M. K., Pomorski, T. G., and Palmgren, M. G. (2010) *Mol. Biol. Cell* **21,** 791–801
19. van der Velden, L. M., Wichers, C. G., van Breevoort, A. E., Coleman, J. A., Molday, R. S., Berger, R., Klomp, L. W., and van de Graaf, S. F. (2010) *J. Biol. Chem.* **285,** 40088–40096
20. Lenoir, G., Williamson, P., Puts, C. F., and Holthuis, J. C. (2009) *J. Biol. Chem.* **284,** 17956–17967
21. Bryde, S., Hennrich, H., Verhulst, P. M., Devaux, P. F., Lenoir, G., and Holthuis, J. C. (2010) *J. Biol. Chem.* **285,** 40562–40572
22. Kwok, M. C., Holopainen, J. M., Molday, L. L., Foster, L. J., and Molday, R. S. (2008) *Mol. Cell Proteomics* **7,** 1053–1066
23. Chomczynski, P., and Sacchi, N. (1987) *Anal. Biochem.* **162,** 156–159
24. MacKenzie, D., and Molday, R. S. (1982) *J. Biol. Chem.* **257,** 7100–7105
25. Chen, C., and Okayama, H. (1987) *Mol. Cell. Biol.* **7,** 2745–2752
26. Bungert, S., Molday, L. L., and Molday, R. S. (2001) *J. Biol. Chem.* **276,** 23539–23546
27. Papermaster, D. S., and Dreyer, W. J. (1974) *Biochemistry* **13,** 2438–2444
28. Molday, L. L., Cook, N. J., Kaupp, U. B., and Molday, R. S. (1990) *J. Biol. Chem.* **265,** 18690–18695
29. González-Romo, P., Sánchez-Nieto, S., and Gavilanes-Ruíz, M. (1992) *Anal. Biochem.* **200,** 235–238
30. McIntyre, J. C., and Sleight, R. G. (1991) *Biochemistry* **30,** 11819–11827
31. Romsicki, Y., and Sharom, F. J. (2001) *Biochemistry* **40,** 6937–6947
32. Krogh, A., Larsson, B., von Heijne, G., and Sonnhammer, E. L. (2001) *J. Mol. Biol.* **305,** 567–580
33. Gupta, R., and Brunak, S. (2002) *Pac Symp Biocomput.* **7,** 310–322
34. Julenius, K., Mølgaard, A., Gupta, R., and Brunak, S. (2005) *Glycobiology* **15,** 153–164
35. Shevchenko, A., Wilm, M., Vorm, O., and Mann, M. (1996) *Anal Chem* **68,** 850–858
36. Perkins, D. N., Pappin, D. J., Creasy, D. M., and Cottrell, J. S. (1999) *Electrophoresis* **20,** 3551–3567
37. Katoh, Y., and Katoh, M. (2004) *Oncol Rep.* **12,** 939–943
38. Osada, N., Hashimoto, K., Hirai, M., and Kusuda, J. (2007) *Gene* **392,** 151–156
39. Xu, P., and Ding, X. (2007) *Acta Biochim. Biophys. Sin.* **39,** 739–744
40. Doi, T., Molday, R. S., and Khorana, H. G. (1990) *Proc. Natl. Acad. Sci. U.S.A.* **87,** 4991–4995
41. Jaunin, P., Jaisser, F., Beggah, A. T., Takeyasu, K., Mangeat, P., Rossier, B. C., Horisberger, J. D., and Geering, K. (1993) *J. Cell Biol.* **123,** 1751–1759
42. Hasler, U., Wang, X., Crambert, G., Béguin, P., Jaisser, F., Horisberger, J. D., and Geering, K. (1998) *J. Biol. Chem.* **273,** 30826–30835
43. Hasler, U., Crambert, G., Horisberger, J. D., and Geering, K. (2001) *J. Biol. Chem.* **276,** 16356–16364
44. Abe, K., Tani, K., Nishizawa, T., and Fujiyoshi, Y. (2009) *EMBO J.* **28,** 1637–1643